

## 300mm IGZO nFETs with low-T Ru contacts for localized doping and increased BEOL compatibility

Luka Kljucar, Quentin Smets, Michiel Setten, Jerome Mitard, Atillio Belmonte, Harold Dekkers, Lieve Teugels, Ming Mao, Harinarayanan Puliyalil, Jose Ignacio del Agua Borniquel<sup>2</sup>, Romain Delhougne, Gouri Sankar Kar, Zsolt Tokai  
imec, Kapeldreef 75, 3001 Leuven, Belgium, Tel: +32 1628 3413, e-mail: [luka.kljucar@imec.be](mailto:luka.kljucar@imec.be), <sup>2</sup>Applied Materials Belgium, APTD, Leuven, Belgium,

### Abstract

**Using our back-gated 300mm integration scheme, we demonstrate Back-End-Of-Line (BEOL)-compatible InGaZnO (IGZO) based nFETs, substituting tungsten (W) with ruthenium (Ru) as our source-drain (S-D) contact material. Compared to W contacts, nFETs with Ru S-D show higher  $I_{on}$ , lower  $I_{off}$ , no negative  $V_{th}$  roll-off, and steeper subthreshold swing (SS). In addition to better electrostatics, short-channel devices with Ru contacts retain their off-state characteristics at the end of processing, omitting the need for extra oxygen anneal. Combined with 325°C Ru deposition temperature, this makes IGZO nFETs with Ru contacts a promising candidate as BEOL transistor for logic and memory applications.**

### 1. Introduction

Recently, IGZO is gaining in popularity as a channel material of choice for emerging BEOL applications. IGZO has several advantages, like higher mobility, high  $I_{on}/I_{off}$  ratio, and low process temperature [1]. While currently most efforts are geared towards improving the IGZO or metal oxide materials to reach levels of maturity necessary for BEOL integration [2,3], in this work we focus on increasing the BEOL compatibility by changing the S-D contact metal by leveraging our 300mm IGZO nFET platform [4]. Simultaneously, we also improve device characteristics of our IGZO nFETs.

### 2. Contact material selection by ab-initio simulations

To guide our contact material selection, extensive ab-initio simulations were performed to determine the oxide formation energy for different IGZO/metal systems. This is crucial for determining IGZO/metal interface stability, as metals which easily oxidize also scavenge O from IGZO. This scavenging can extend over several hundreds of nm, which n-dopes the entire channel and prevents device turn-off.

Fig.1 shows industry-standard W has very negative oxide formation energy and therefore scavenges O from IGZO. We identify Ru as a good candidate with less negative oxide formation energy. Ru can also be integrated using a standard BEOL damascene scheme, has a low thermal budget, and it does not require a thick dielectric barrier.

### 3. Device fabrication

Therefore, we benchmark our POR process with W against Ru. The devices are fabricated using our 300mm back-gated integration scheme outlined in our previous work [4]. Following the deposition of back gate dielectrics (5nm SiCN and 15nm Al<sub>2</sub>O<sub>3</sub>) and amorphous 12nm IGZO, we form the IGZO active area using a combination of Reactive Ion Etch (RIE) and Ion Beam Etch (IBE). This is followed by

dielectric fill and planarization. S-D contacts are patterned using industry-standard damascene scheme. Two metallization schemes were used. For the W scheme, we deposit 6nm ALD TiN, followed by ALD/CVD W fill and CMP. For the Ru scheme, we deposit ALD TiN of varying thickness (either 6nm, 1nm, or 0.3nm) followed by 2nm ALD Ru, which serves as a nucleation layer. This is followed by CVD/PVD Ru fill and Cu plating used to assist with the final planarization step. The SEM images of final device can be seen in Fig. 2. The device channel length ( $L_{ch}$ ) is defined by the S-D contact distance.

### 3. IGZO nFET assessment

A first screening of the devices is done immediately after last CMP step, where we assess devices with  $L_{ch}$  ranging from 32.2 $\mu$ m down to 245nm. With the absence of O<sub>2</sub> anneal, devices with W contacts show degraded off-state, irrespective of the channel length, as shown in Fig. 3. Here, we are seeing only saturation portion of the I-V curve, as the IGZO is in a highly doped state. On the other hand, devices with 6nm TiN+Ru contacts do show modulation, where we see a trend of improved off-state characteristics with reduced channel length. This indicates that, compared to W-filled contacts, the doping with Ru contacts is more localized, and less additional oxygen vacancies are created in the channel area. In addition to the remote scavenging of the W-fill contacts, extra H<sub>2</sub> doping during W deposition may also contribute to degraded off-state after full processing, especially for long channel devices.

However, the more localized O<sub>2</sub> scavenging by Ru contacts and resulting off-state retention depends on the thickness of the TiN barrier. As the TiN barrier is reduced from 6nm, to 1nm, to 0.3nm (non-continuous layer), the off-state degradation increases, as shown in Fig. 4. This means that a correct thickness of barrier material is also essential to reach the correct doping levels in the channel, and therefore optimal device behavior.

After the initial screening, we perform a 1hr anneal at 350°C in O<sub>2</sub> atmosphere, and again assess the devices. This time, we do see modulation for devices with W contacts, because oxygen vacancies have mostly been passivated. However, compared to Ru devices with same TiN thickness after O<sub>2</sub> anneal, we still see higher non-uniformity, and up to -1V negative  $V_{th}$  roll-off, which is shown in Fig. 5. Interestingly, we also now observe that devices with Ru contact have no  $V_{th}$  shift, irrespective of the channel length. This shows that for long channel devices, O<sub>2</sub> anneal is still necessary to passivate the oxygen vacancies to reduce the overall doping levels. For short channel devices this is not necessary, as O<sub>2</sub> scavenging from Ru contacts is sufficiently localized, and the channel

area is small enough not to be excessively doped by subsequent processing. Comparing W and 6nm TiN+Ru devices in Fig. 6, we see that 6nm TiN+Ru contacts have the highest  $I_{on}$  ( $3\times$  higher than TiN+W contacts), lowest  $I_{off}$  below the noise floor (1pA/ $\mu\text{m}$ ), no negative  $V_{th}$  roll-off and best SS (120mV/dec vs 175mV/dec for smallest devices).

#### 4. Conclusions

We demonstrate that W-based contacts strongly scavenge O from IGZO, and dope the entire channel, while Ru contacts only locally dope the channel. Therefore, all device characteristics show improvement with Ru contacts, both before and

after  $O_2$  anneal. In addition, we see that for short channel devices with Ru contacts, we can omit final oxygen anneal, and therefore increase compatibility with standard low-T BEOL integration schemes.

#### References

- [1] S. Yamazaki *et al.*, *JJAP* (2014), Vol 45, Nr. 4S
- [2] W. Chakraborty *et al.*, *VLSI* (2020).
- [3] S. Samanta *et al.*, *VLSI* (2020).
- [4] L. Kljucar *et al.*, *SSDM* (2019), pp, 303-304.

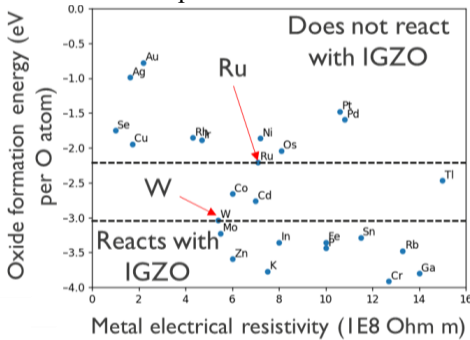


Figure 1. Oxide formation energies for different contact metals

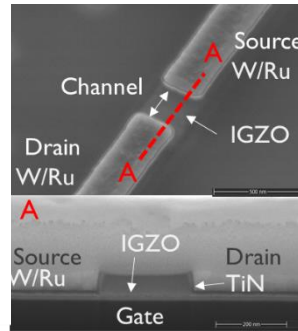


Figure 2. FIB SEM of the device

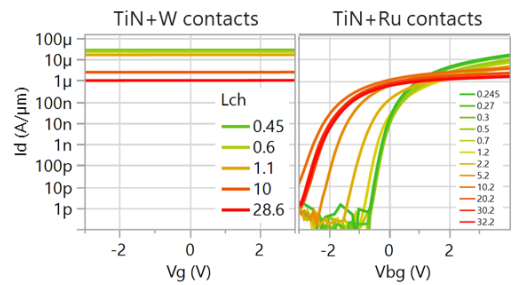


Figure 3.  $I_d$ - $V_g$  curves of IGZO nFETs with W and Ru contacts (6nm TiN thickness both), post processing and pre oxygen anneal

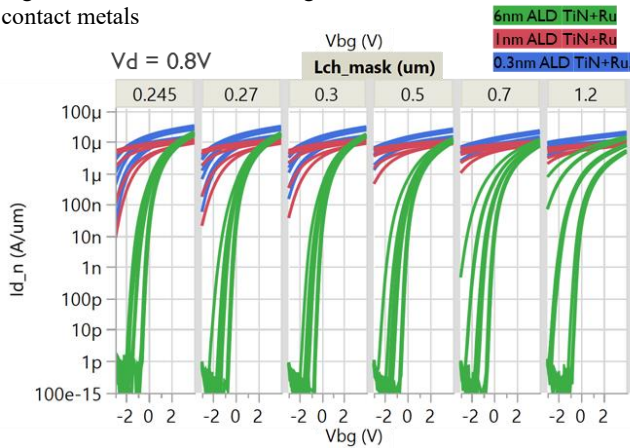


Figure 4. Impact of TiN thickness on IGZO nFET characteristics with Ru contacts after device processing, before  $O_2$  anneal

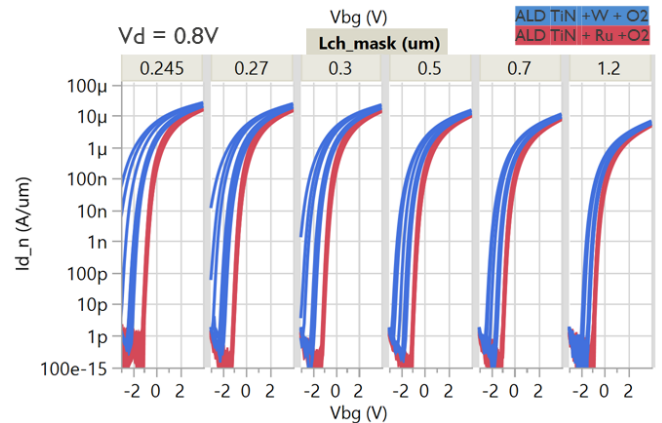


Figure 5. Comparison of  $I_d$ - $V_g$  curves of IGZO nFET with W and Ru contacts after  $O_2$  anneal

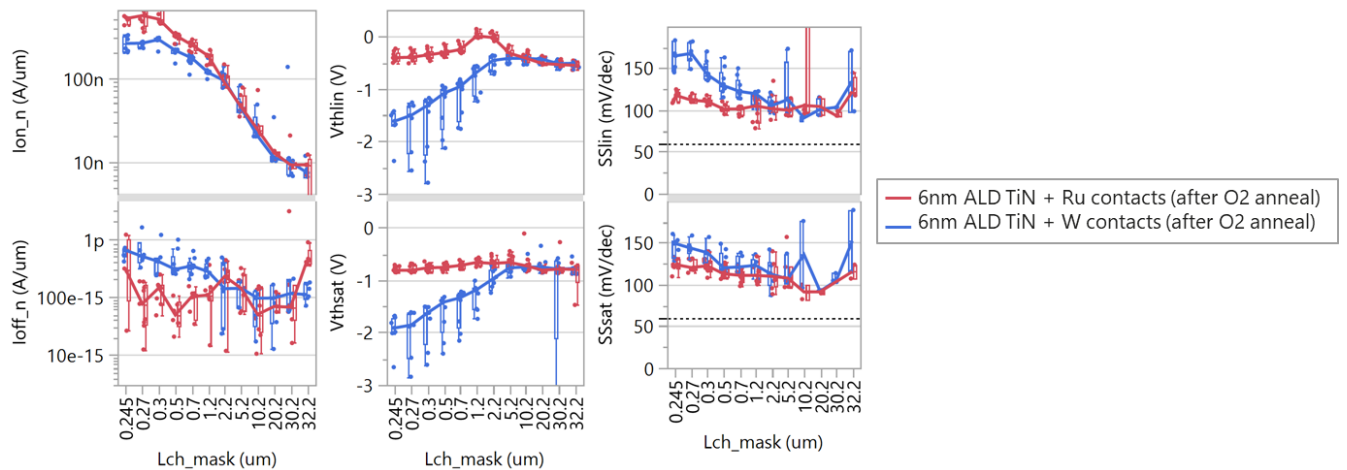


Figure 6. IGZO nFET device performance after oxygen anneal for different contact schemes